

Synthesis, Morphology, and Melting Behavior of Poly(ether ether ketone) of Different Molecular Weights

Qianshu Lu,¹ Zhenguo Yang,¹ Xiaohui Li,² Shilei Jin²

¹Department of Materials Science, Fudan University, Shanghai 200433, People's Republic of China

²Department of Polymer Engineering, Shanghai Research Institute of Materials, Shanghai 200437, People's Republic of China

Received 12 December 2008; accepted 16 May 2009

DOI 10.1002/app.30786

Published online 30 June 2009 in Wiley InterScience (www.interscience.wiley.com).

ABSTRACT: To investigate how the molecular weight of poly(ether ether ketone) affected the crystallization behavior, the nucleophilic reaction synthetic technology was used to obtain poly(ether ether ketone) of different molecular weights and the trend of the molecular weight varying with the duration of the reaction. Furthermore, the influence molecular weight has brought to the morphology and the melting behavior was investigated by means of FTIR, OM, WAXD, and DSC and thoroughly discussed in theory. Results showed that with the increase of the molecular weight, the degree of crystalline perfection and the

lamellar thickness descended as well as the radius of spherulite diminished due to the difficulty of the chain mobility. Moreover, the melting temperature mounted up at first then decreased with the growing of the molecular weight indicating how the lamellar thickness and the melting heat per unit volume affected the melting behavior together. © 2009 Wiley Periodicals, Inc. *J Appl Polym Sci* 114: 2060–2070, 2009

Key words: PEEK; molecular weight; synthesis; morphology; melting point

INTRODUCTION

Poly(ether ether ketone) (PEEK) is a semicrystalline and high-temperature aromatic polymer with good thermal and mechanical properties combined with excellent chemical resistance.^{1–3} PEEK has an outstanding thermal resistance. It can persist for a long time under 250°C. The momentary using temperature can reach 300°C. When the temperature reaches 400°C, PEEK can remain stable without decomposing.⁴ Moreover, there are series of mechanical advantages of PEEK such as high strength, high toughness, high wear resistance, and excellent dimensional stability.⁵ The excellent chemical resistance of PEEK that can only dissolve in oil of vitriol is also notable. Since PEEK has a broad applications as a result of its highly desirable properties including good processability, excellent high mechanical strength, and stability in many harsh environment,⁶ a lot of publications have devoted to its synthesis methods, crystallization, and melting behavior as well as the morphology.

Generally speaking, there are two main synthetic methods of PEEK: the nucleophilic polycondensation and the electrophonic polycondensation.⁷ In the case

of nucleophilic reaction, 4,4'-fluoride benzophenone and hydroquinone have condensation reactions at the presence of alkali metal carbonate used as catalyst and diphenylsulfone used as solvent. The reaction temperature should reach 280–340°C, which is relatively high. John and Philip⁸ invented this synthetic way above and organized all aspects of study to investigate how the ratio of K₂CO₃ and Na₂CO₃ influenced the molecular weight distribution. In their research, one special part focused on the influence on the molecular weight by the reaction time indicating that the molecular weight mounted up with the increase of the reaction time which was one of the bases of our study. The side reaction can be easily controlled in the nucleophilic reaction method, but the technology is far more complicated and has quite a high cost.⁹ In contrast, the electrophilic reaction which diphenylether and meta-dimethyl benzene chloride synthesize under the normal temperature can occur at a more gentle condition and the cost is low. However, the side reaction in this reaction system is hard to control, which affects the output and the quality of the PEEK products deeply. So the nucleophilic method has been widely used in the industry by ICI since 1977 instead of the electrophilic way. By the way, the fully amorphous state of PEEK is formed by quenching from the melt while the maximum crystallization can be produced by annealing from the melt.¹⁰

Over the last two decades, to accommodate the enormous applications, the crystallization and

Correspondence to: Z. Yang (zgyang@fudan.edu.cn).

Contract grant sponsor: Shanghai Leading Academic Discipline Project; contract grant number: B113.

melting behavior have been studied extensively via differential scanning calorimetry (DSC),^{11–16} small-angle X-ray scattering (SAXS) and wide-angle X-ray diffraction (WAXD),^{17–24} thermomechanical analysis,^{25–27} transmission electron microscopy (TEM),^{28,29} and optical microscopy (OM).^{20–33} The process of bulk crystallization of PEEK was studied through the separation of the nucleation and growth steps by Medellin-rodriguez and Phillips.³⁴ It was observed that a first slope at low crystallization times is associated with massive heterogeneous nucleation and/or local-order-promoted primary nucleation of spherulitic crystal. A second gradual decrement in intensity follows, showing a logarithmic tendency. These are associated with the end of the process of crystallization of primary spherulites and in large proportion the nucleation and growth, at lower rates, of sporadically nucleated spherulites. Ivanov et al.³⁵ found two regimes of reorganization behavior evidenced in their study. In the low temperature interval (temperatures below $T_g + \sim 50$), the slow dynamics of amorphous segments prevents large-scale rearrangements, strongly limiting the process of reorganization. At higher temperatures, however, a larger-scale melting/recrystallization mechanism sets in. It consists in the recrystallization of whole lamellar stacks to give a state of overall lower free energy, with much thicker and dense crystals separated by larger and less constrained amorphous region of lower T_g . Recrystallization through the final melting region of PEEK was confirmed by William and Bryan³⁶ via temperature modulated DSC (TMDSC) over a broad range of annealing times and temperatures. In the aspect of morphology study of PEEK, Yongsok and Sehyun³⁷ provided valuable information about the crystal structure and morphology by their study of nonisothermal crystallization behavior of PEEK. As a consequence of heating to above their normal melting temperature, the morphology of PEEK changes dramatically.⁶

As the consequence of the large amount of pertinent research, people became to know more about PEEK and make proper and broad applications with it. Especially in nowadays industrial development, higher specific strength and more environmental friendship led to PEEK being adopted for use in many fields instead of metals. So it is necessary to have an all-around study on the practical properties of PEEK. Many articles have put forward that the thermal and mechanical properties were found to be strongly dependent on the molecular weight for polydisperse industrial PEEK samples.^{38–40} But

except for the work done by Fougins et al.¹⁰ which only focused on the melting behavior of narrow molecular weight fraction of PEEK annealed from the glassy state, few studies were devoted to the influence of the molecular weight of PEEK on its properties. Accordingly, the present work gives a wholly study while focusing on the synthesis method of different-molecular-weight PEEK as well as the evolutions of the morphology and the melting behavior versus molecular weight of the PEEK products obtained from the synthesis procedure annealing from the melt by means of FTIR, DSC, WAXD, and OM. Since PEEK has a good chemical resistance, it can dissolve in concentrated sulfuric acid. So, the intrinsic viscosity was chosen to characterize the molecular weight in this article instead of measuring by GPC which has a strict impregnant restriction.

EXPERIMENTAL SECTION

Materials and sample preparation

The hydroquinone was obtained from Sinopharm Chemical Reagent (SCRC). It was recrystallized in acetone under the protection of N_2 and dried under the vacuum condition at 60°C.

The 4,4'-fluoride benzophenone which was produced for industry was taken from Changzhou Huashan Chemical. It was recrystallized by methanol and dried under the vacuum condition at 65°C.

Both of the anhydrous potassium carbonate and the anhydrous sodium carbonate produced for research were obtained from Sinopharm Chemical Reagent (SCRC). They were carefully dried at 100°C before use.

The purity of the diphenylsulfone taken from Nanjing Shengqi Chemical reached 98%. It was necessary to be recrystallized by acetone and dried under the vacuum condition at 60°C.

The acetone and methanol used as the solvent in the recrystallization procedure was produced by Shanghai Chemical Reagent and Sinopharm Chemical Reagent, respectively.

The physical parameters of the main reagents were listed in Table I.

Synthesis

The present work used the nucleophilic reaction synthetic technology with 4,4'-fluoride benzophenone and hydroquinone in the presence of alkali metal carbonate as catalyst and diphenylsulfone as solvent to synthesize PEEK.

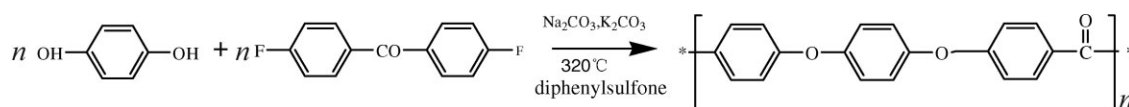


TABLE I
Physical Parameters of the Main Reagents

Name\performance	Molecular formula	Molecular weight	Density (g/cm ³)	Melting point (°C)	Boiling point (°C)	Remark
4,4'-Fluoride benzophenone	C ₁₃ H ₈ F ₂ O	218		106–109	137	
Hydroquinone	C ₆ H ₆ O ₂	110	1.332	172	286	Flash point 165°C
Diphenylsulfone	C ₁₂ H ₁₀ O ₂ S	218		125–129	379	
Acetone	C ₃ H ₆ O	58	0.79	–95	56	
Anhydrous sodium carbonate	Na ₂ CO ₃	106	2.532	851		
Anhydrous potassium carbonate	K ₂ CO ₃	138	2.428	891		

4,4'-fluoride benzophenone (117.46 g, 0.54M), hydroquinone (59.27 g, 0.54M), and diphenylsulfone (323.27 g, 1.48M) were charged to a 250-mL four-necked glass flask equipped with a stirrer, nitrogen inlet, condenser, and a thermometer. When wholly protected by N₂, these materials was heated with stirring gradually to 180°C to form a nearly colorless solution and, containing a nitrogen blanket, anhydrous potassium carbonate (3.72 g, 0.027M) and anhydrous sodium carbonate (55.49 g, 0.52M) was added. The temperature was raised to 200°C and maintained there for 1 h; the temperature then raised to 250°C and maintained there for 1 h; finally the temperature raised to 320°C and maintained there for 0.5, 1.5, 2.5, 3.5, and 4.5 h, respectively, the resulting polymers being in solution at this stage. In the normal temperature, raved about the hot mixture immediately to a plate in the 25°C water. The mixture was rapidly cooled and the resulting solid reaction products were milled. Diphenylsulfone and inorganic salts were removed by washing successively with acetone (twice), water (twice), and acetone (twice). The resulting polymers were dried at 120°C.⁸

Measurements

FTIR

Structural characterization of sulfonated polymer was done by FTIR.⁴¹ The 4.5 h PEEK sample using KBr pellet was recorded on PARAGON10001 spectrometer which was produced by Peakin Elmer.

Intrinsic viscosity measurement

Intrinsic viscosities of PEEK products were obtained by measurements with Ubbelohde viscometer of 0.9–1.0 mm and a series of operations.^{8,42,43} Intrinsic viscosity in this article was measured at 25°C on a solution of the polymer in concentrated sulfuric acid of density 1.84 g/cm³, said solution containing 0.1 g of polymer per 100 cm³ of solution. Then, the average flowing times of the concentrated sulfuric acid (t_0) and the solvent of the five samples (t) which were ~ 2 min were measured by the Ubbelohde viscometer, respectively. The relative viscosity (η_r) can be obtained by the formula: $\eta_r = t/t_0$, then we can get

the reduced viscosity ($\frac{\eta_{sp}}{C} = \frac{\eta_r - 1}{C}$). On the basis of the definition of the intrinsic viscosity, $[\eta] = \lim_{C \rightarrow 0} \frac{\eta_{sp}}{C} = \lim_{C \rightarrow 0} \frac{\ln \eta_r}{C}$, $\frac{\eta_{sp}}{C}$ and $\frac{\ln \eta_r}{C}$ were ascertained as ordinate as well as the concentration (C) was deemed as abscissa to create two lines. When C was equal to 0, their intercept were definitely the intrinsic viscosity. The results of this article belonged to $k < 1/3$ (k is a constant be foreign to the condensations, representing some uncertain physical meaning including the hydrodynamics and the thermodynamic items), in other words, the $\frac{\ln \eta_r}{C} - C$ were curves bending at the high condensation interval instead of straight lines. The tangents of the curves with slopes (β) according with $\beta < 1/2 - k$, were intersected with the $\frac{\eta_{sp}}{C} - C$ line at the interval of $C < 0$. Here, the tangents of the Huggins equation $\frac{\eta_{sp}}{C} = [\eta] + k[\eta]2C$ ($k[\eta]C \ll 1$) were deemed as the intrinsic viscosity in this article.

Wide angle X-ray diffraction

D/max- γ B produced by RIKAV was used to detect the crystal structure of PEEK.^{44,45} The range of scattering angle was $5.00 < 2\theta < 90.00^\circ$ and the scanning rate was $6.00^\circ/\text{min}$. It should be noted that the intensity (I) represented by the peak height pointed the distance between the baseline and the steeply-crowned point of the diffraction. Meanwhile, full width at half maximum (FWHM) referred to the width of the half height peak. Here, we created a value to present the composite influence of the intensity and FWHM called the degree of acumination (DA) obtained by $DA = I/\text{FWHM}$. We can also get lamellar thickness (L_{hkl}) of the five samples from this measurement by the Scherrer function: $L_{hkl} = \frac{k\lambda}{\beta \cos \theta}$. L_{hkl} was the average lamellar thickness vertical to the crystal plane (hkl); λ was the wavelength of the X-ray; θ was the Bragg angle; and the β represented the diffraction linewidth. When the diffraction linewidth was ascertained as the FWHM, k equaled to 0.89.

Optical microscope

The optical microscope produced by Shanghai Optical equipment was used to take the micrograph of the crystal of the PEEK samples.⁴⁶

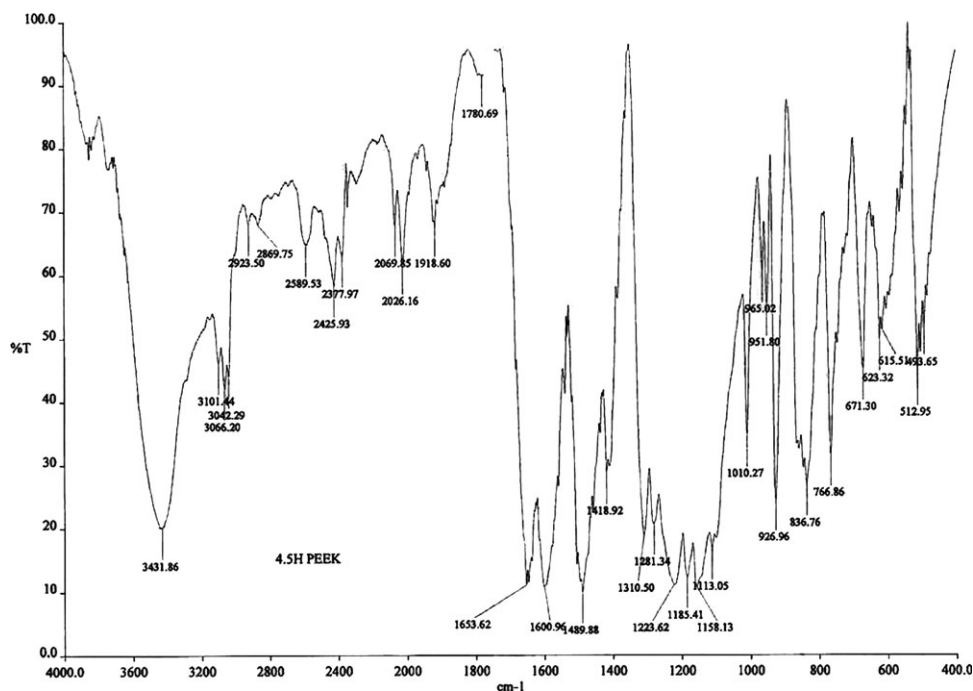


Figure 1 FTIR spectra of PEEK (4.5 h).

Differential scanning calorimetry

The DSC measurements were made by Peakin Elmer DSC-6 differential scanning calorimeter operating at a heating rate of 10°C/min in a heat flux differential scanning calorimeter working under nitrogen atmosphere.⁴⁷ The scanning scope was 50.0–380.0°C.

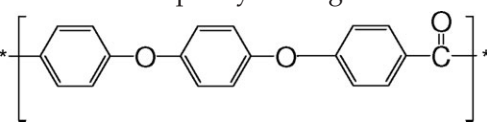
RESULTS AND DISCUSSION

White and gray solid carried out at the durations of reaction 0.5, 1.5, 2.5, 3.5, 4.5 h, respectively were obtained as samples. Firstly, FTIR was used to confirm that the synthesis products were PEEK. On the basis of the affirmance, intrinsic viscosity measurement, WAXD, OM, and DSC were taken in order to get informations about the morphology and melting behavior of PEEK varying with their molecular weights.

Structural validation

Figure 1 showed the spectra corresponding to the PEEK sample whose duration of reaction was 4.5 h. It had an absorption peak at 1653.62 cm⁻¹ due to C=O stretch. The bands at 1600.96 and 1489.88 cm⁻¹ were assigned to in-plan vibrations of benzene ring of R–O–R as well as 1310.50 cm⁻¹ was engendered by R–CO–R in-plan vibration of benzene ring. In addition, the absorption at 1223.62 cm⁻¹ was the asymmetric R–O–R stretch of aromatic compounds. The absorptions observed at 1185.41, 1158.83,

1113.05, 1010.27 cm⁻¹ were the C–H in-plan bending of aromatic ketone or aromatic ether. The C–H out-of-plan bending of benzene was characterized by the absorption peak at 836.76, 766.86 cm⁻¹. Furthermore, the 836.76 cm⁻¹ peak also represented the p-substitute of phenyl ring. In conclusion,

the  structure existed.

The synthetic method of the PEEK with different molecular weight and the probable microcosmic movement

Figure 2 showed the intrinsic viscosity of the five PEEK samples obtained from the Ubbisich viscometer measurement. Obviously, the $[\eta]$ increased with the reaction time from 0 to 3.5 h and leveled off above 3.5 h. It should be noted that in the interval of 0 to 3.5 h, the intrinsic viscosity increased dramatically especially from 2.5 to 3.5 h. However, above 3.5 h, the change of $[\eta]$ was not sufficient severity to the evolution of the reaction time. Furthermore, the final increase of the $[\eta]$ gradually increased and in the end reached 1.325. From the Mark-Houwink's formula:

$$[\eta] = KM^\alpha,$$

in which K was a constant as well as α referred to the expansion factor related to the morphology of

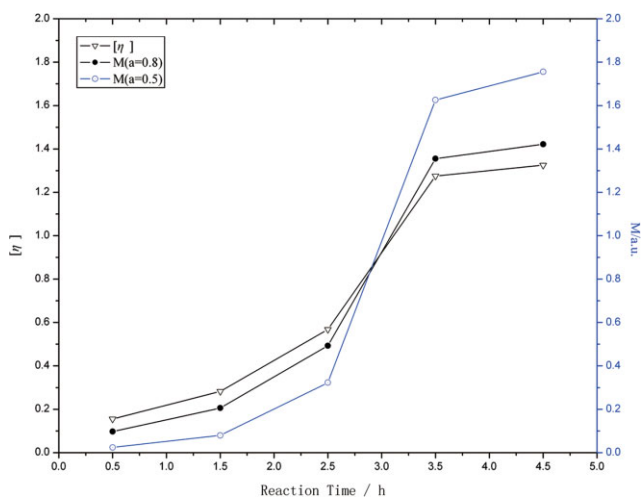


Figure 2 The variation of intrinsic viscosity and the extremum molecular weight with the reaction time. [Color figure can be viewed in the online issue, which is available at www.interscience.wiley.com.]

the polymers in the solution, we can extrapolate that $M = ([\eta]/K)^{1/\alpha}$.

In addition, for most flexible polymers, α is equal to a value between 0.5 and 0.8. Consequently, when we let α be 0.5 and 0.8, respectively, the critical trends of molecular weight varying with the reaction time was obtained (Fig. 2). The extremum molecular weight was also monotonically rising throughout the duration of the reaction from 0 to 3.5 h. However, when the reaction time was above 3.5 h, the increasing trends of the extremum molecular weight became unobvious as well as the tail ends reached constants, respectively.

Result of the intrinsic viscosity measurements indicates the evolution of the molecular weight and the intrinsic viscosity with the increase of the reaction times. As the duration of reaction increases, a number of effects become apparent, and in discussing these it is convenient to divide the trends in Figure 2 into three groups on the basis of their slopes. Below the 2.5 h, the changes are gradual for reason that the monomers firstly become dimmers and oligomers before coming

into being polymers according to the mechanism of the condensation reactions. When the dimmers continue to condense to become polymers, moreover, under the same temperature, it needs some time for the end groups of the polymer chains to diffuse in order to encounter and react. Therefore, as the reaction time increases, one period of time, from 2.5 to 3.5 h, with largest encountering probability of end groups is ascertained, while the intrinsic viscosity and the extremum molecular weight increasing dramatically. However, above 3.5 h, the changes of $[\eta]$ are not sufficient severity to the evolution of the reaction time as well as the final $[\eta]$ reaches to 1.325. This is because of the limited content of the materials in the synthetic system. Suppose that the reaction time is long enough as well as the molecular weight also came to a high level, in other words, the number of the end groups is limited for reason that most of them have already condensed into long chains. Meanwhile, the viscosity of the synthetic system increases corresponding to the molecular weight. Consequently, it is quite difficult for the long chains to move effectively for further condensation. At this moment, the increase of the molecular weight is confined and the trends level off and potentially approach to a constant in the end of the reaction for the reasons above. Based on the above interpretations, we image a microscopic synthetic procedure (Fig. 3).

It can be extrapolated that the duration of reaction should be seriously chosen in order to get the products of relatively high molecular weight. However, the optimization of the reaction time depends on the idiographic condensation system. For example, to the system in this article, we deem 3.5 h as the proper time for condensation.

Under the normal condition, PEEK can only dissolve in concentrated sulfuric acid. So, GPC and other normal measurement cannot give the exact value of the molecular weight baffled by the impregnant problems. However, in Figure 2, concomitant with the trends of molecular weight, intrinsic viscosity is ascertained to be used for the further discussions of the morphology and melting behavior instead of the molecular weight.

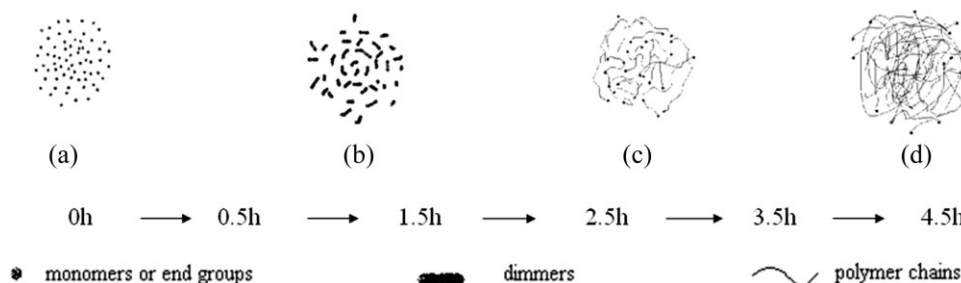


Figure 3 Microscopic synthetic procedure of PEEK.

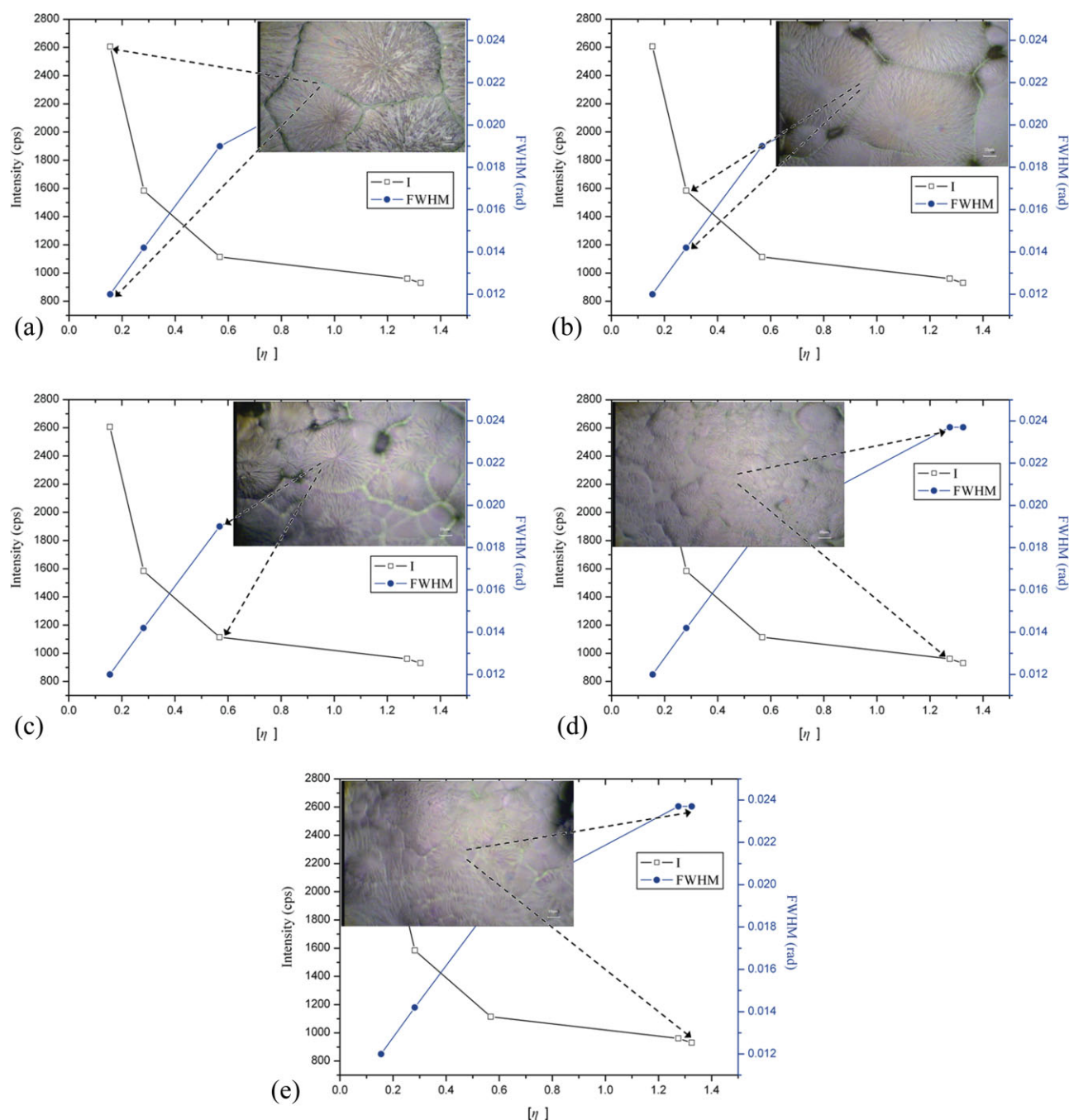


Figure 4 Contrast between the trends of the peak height and the FWHM of (110) fraction and the optical micrographs of (a) 0.5 h; (b) 1.5 h; (c) 2.5 h; (d) 3.5 h; (e) 4.5 h PEEK samples. [Color figure can be viewed in the online issue, which is available at www.interscience.wiley.com.]

Relationship between the morphology and the molecular weight of PEEK

The variation of the morphology of PEEK versus molecular weight could be observed by means of WAXD and OM. The results from the two kinds of measurements are in agreement (Fig. 4).

The decrease of the degree of crystal perfection is detected, which could be accounted for by variation in the coherence of the degree of acumination of (110) diffractions from WAXD. The main peak of the

(110) diffractions were very close to those already published by Rao et al.⁴⁸ PEEK belonged to orthorhombic system and "Pbcn" space group which had four crystallization peaks whose 2θ were 18.76° , 20.62° , 22.90° , and 28.80° , respectively (Fig. 5). From the function $d = \lambda_{X\text{-ray}}/2\sin \theta$,⁴³ the interplanar crystal spacing was obtained as 0.472, 0.430, 0.388, and 0.310 nm, respectively. It should be noted that the 2θ of the peaks of the WAXD reflection were not influenced by the molecular weight indicating that the

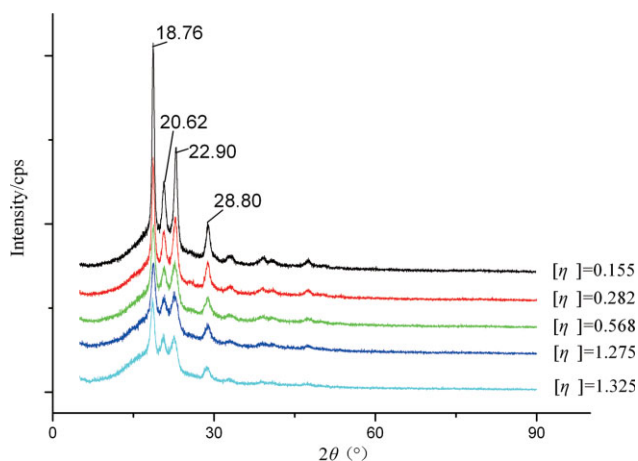


Figure 5 WAXD pattern of the five PEEK samples. [Color figure can be viewed in the online issue, which is available at www.interscience.wiley.com.]

crystal structure type remained the same despite the changes of the molecular weight. In addition, the FWHM of the (110) diffraction augmented and the intensity decreased with increasing molecular weights (Fig. 6), indicating a higher inner stress, smaller dimension and lower degree of crystal perfection of the crystals. Moreover, the plots of the 3.5 and 4.5 h PEEK samples in the trends of intensity and FWHM versus intrinsic viscosity (Fig. 6) were nearly the same mainly because of their approximate intrinsic viscosities. The degree of acumination of the five PEEK samples obtained by means of the equation given in Experimental section, roughly corresponded to the trends of the peak height of the (110) diffraction or, equivalently, to the decrease of the FWHM of the (110) diffraction versus intrinsic viscosity. The decreased degree of acumination also indicated a higher inner stress, smaller dimension, and lower degree of crystal perfection of the crystals, which were usually more sensitive to the change in the molecular weight. The lamellar thicknesses of the five samples decreased with the molecular weight. The largest average lamellar thickness belonged to the 0.5 h sample which was 11.59183 nm. It was nearly twice of the smallest ones belonged to the 3.5 and 4.5 h samples.

As stated in the results above for the case of WAXD, the evolution of the peak height and FWHM indicates a higher inner stress, smaller dimension, and lower degree of crystalline perfection of the crystals because of the enhanced intrinsic viscosity which baffles the movements of the polymer chains for orderly arrangement. Accordingly, the nearby segments are inclined to intertwine. This can be perfectly validated by the similarity of the peak height and FWHM between 3.5 and 4.5 h samples due to their approximate intrinsic viscosity (Fig. 6), indicating the similar mobility of nearby segments which

determine the analogical inner stress, crystal dimension as well as the approximative degree of crystalline perfection. It should be noted that the 2θ of the peaks of the WAXD reflection were not influenced by the molecular weight indicating that the crystal structure type remained the same despite the changes in the molecular weight.

The radius and the dimensions of the spherulites from optical microscopy experiments performed on crystals of PEEK samples are in a full agreement with the interpretation presented in the above paragraph (Fig. 4). The optical studies showed that the crystals of PEEK were spherulites³³ with emanant radial growing fibers that were composed of long strip lamellar crystals [Fig. 7(a)]. Among the five samples, one observed that the crystal of 0.5 h PEEK sample had the highest degree of crystalline perfection and the largest radius of the spherulites (Fig. 7). As the molecular weight was growing, the degree of crystalline perfection decreased as well as the radius of the spherulites became smaller. Meanwhile, the arrangement of the crystal became snatchy but the crystal shapes were less anomalous. It should be noted that the radius of the spherulites and the degree of crystalline perfection of the 3.5 h PEEK and the 4.5 h PEEK were nearly the same in respect that their molecular weight were correspondingly similar as well as the movements of their chains [Fig. 7(e,d)].

A briefly accepted interpretation of the growing process of spherulites points out the long strip lamellar crystals grow emanantly to the radial direction at the same speed occurred by the ceaselessly forked growth for the plunge of the impurities. In the case of a limited space, the rapidly increasing crystal dimensions finally make the interfaces anomalous instead of the spherical interfaces⁴¹ as evidenced by Figure 7(a). Taking into account the interfaces of two neighbor crystals of low molecular

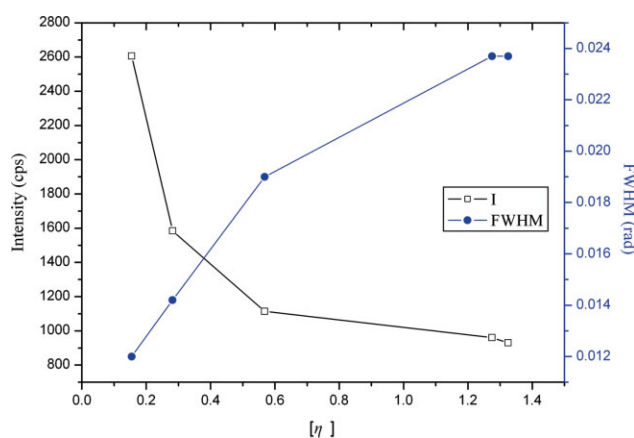


Figure 6 FWHM and the peak height of (110) diffraction for PEEK samples. [Color figure can be viewed in the online issue, which is available at www.interscience.wiley.com.]

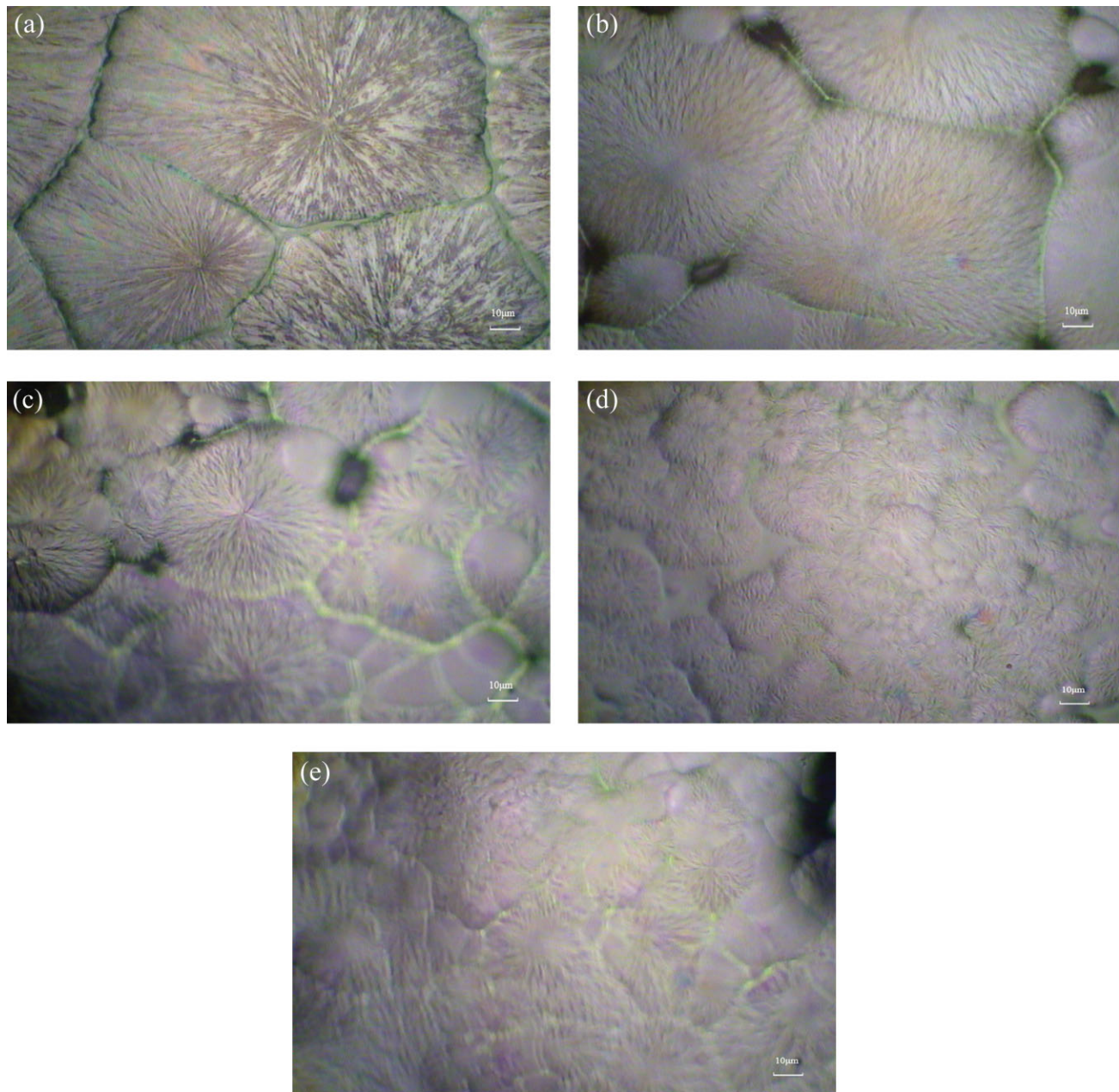


Figure 7 Spherulites morphology of (a) 0.5 h; (b) 1.5 h; (c) 2.5 h; (d) 3.5 h; (e) 4.5 h PEEK samples. [Color figure can be viewed in the online issue, which is available at www.interscience.wiley.com.]

weight samples, there are planes vertical to the line connectings of these two crystal cores which can be another support to the existence of spherulites rather than any other kinds of crystals,⁴¹ although their shapes are anomalous. Moreover, the anomalistic interface of the low molecular weight samples indicates a high growing speed of crystals. In contrast, if there are lots of crystal nucleus and the crystal growing speeds are not fast enough, the crystal dimensions usually appear smaller and have spherical interfaces. Concomitant with the increase of molecular weight, the spherulite diameters turns smaller because of the low growing speed occurred

by the decreasing mobility of the nearby segments. It should be noted that the high molecular weight samples seem having more crystal nucleus in the same area also because of the difficult mobility of the nearby segments which is propitious to the stabilization of crystal nucleus. As a result, the crystal shapes of high molecular weight samples are more inerratic, in other words, their spherical interfaces are more obvious than that of the low molecular weight samples. Corresponding to the similarity of the peak height and FWHM of (110) diffraction of WAXD between 3.5 and 4.5 h samples [Fig. 4(d,e)], the morphology of their crystals are nearly the same

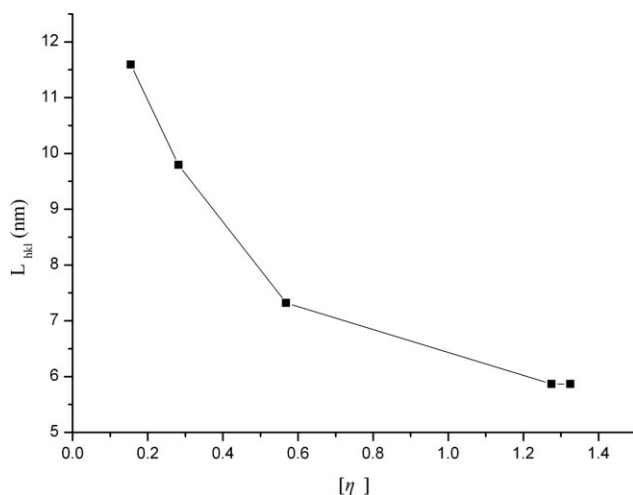


Figure 8 Lamellar thickness versus intrinsic viscosity.

which can be another circumstantial evidence of the above interpretations.

The dramatic variation of the lamellar thickness of the five samples with the molecular weight is another perfect circumstantial evidence to the exploration of the evolution of the degree of the crystal perfection and the radius of the spherulites versus molecular weight above. As the molecular weight increases, the lamellar thickness dramatically decreases from 11.59 to 5.87 nm, indicating the enhanced difficulty of the crystallization and more discontinuousness of crystalline zones in the structure of the spherulites. The long strip lamellar crystals growing emanantly to the radial direction turn to thinner with the increasing molecular weight because of the reduced mobility of the polymer chains. In another aspect, the results also validate the trend of melting temperature with molecular weight in the following paragraph. Meanwhile, we can give a trend (Fig. 8) of the lamellar thickness with the intrinsic viscosity to be a reference of the following studies.

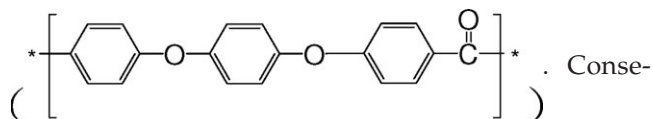
In conclusion, the growing of the crystal is more difficult with the augment of the molecular weight. This can be of great importance for the interpretation of the thermal and mechanical properties of PEEK which have different molecular weights and, in particular, for the understanding of the different applications.

Relationship between the crystallization behavior and the molecular weight of PEEK

The trend in Figure 9 indicated that the evolution of the T_m increased first then decreased with the change of molecular weight. As the molecular

weight increased, a number of effects became apparent, and in describing these it was convenient to divide the samples into two groups on the basis of the monotonicity of the T_m trend. T_m was enhancing at the range of $[\eta]$ being 0.155 to 0.282 and decreased when the $[\eta]$ was above 0.282 shown in Figure 9. Although in this case the melting temperature of $[\eta] = 0.282$ sample was highest, this cannot prove itself the extremum among all the melting temperature of PEEK with intrinsic viscosity at the range of 0.155 to 1.325. Rather, more samples should be prepared and measured by DSC in order to approach the real extremum of T_m over this intrinsic viscosity range.

The trends of melting temperature with molecular weight investigated here are nearly the same to those already published by Fougny.¹⁰ Although the five samples have different molecular weight, their molecular structure are same



quently, they have the same tacticity indicating they can overlap their chains at the same difficulty. Therefore, it can be extrapolated that the variation of T_m is mainly caused by the difference in the chain lengths. Meanwhile, from the theory created by J.I. Lauritzen and J.D. Hoffman: $T_m = T_m^0(1 - 2\sigma_e/l\Delta h)$,⁴¹ in which Δh means melting heat in unit volume; σ_e represents the fold surface energy per unit area; T_m^0 is the melting temperature when the lamellar thickness is ∞ . As the molecular weight increased, a number of effects become apparent, and in discussing these it is convenient to divide

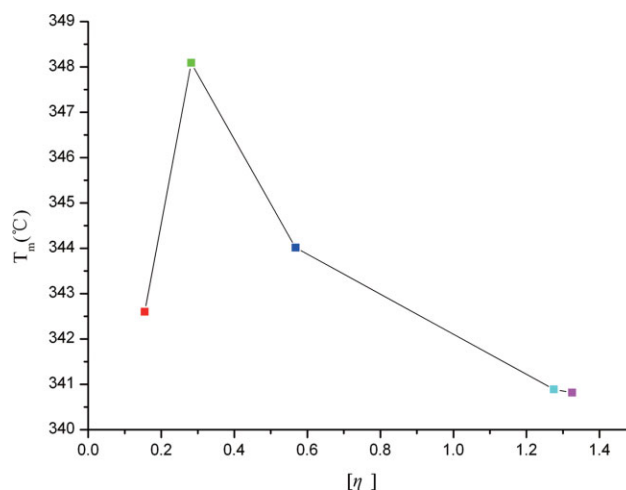


Figure 9 The variation of the melting temperature with $[\eta]$. [Color figure can be viewed in the online issue, which is available at www.interscience.wiley.com.]

the samples into two groups on the basis of the monotonicity of the T_m versus molecular weight. In the increasing interval, it is supposed that although the lamellar thickness is the largest (Fig. 8) as well as the crystalline perfection is highest (Fig. 4), the molecular weights are too low so that the chain segments are too short and apt to start moving which reduce the melting heat in unit volume (Δh) to an adequately low level, bringing on the relatively low T_m of 0.5 h PEEK samples. In contrast, in the decreasing interval, the chain mobility is certainly restricted by the high viscosity caused by large molecular weight which baffles the forming of perfect crystal with large lamellar thickness while also results in a relatively high Δh . So, the melting temperature descends with increasing molecular weight. Generally speaking, the melting heat in unit volume (Δh) and the lamellar thickness (l) influence the T_m together.

CONCLUSIONS

The morphology and melting behavior of PEEK were found to be strongly dependent on its molecular weight while molecular weight was quite influenced by reaction time of the synthesis. Mainly, the crystalline process was found to be hindered by the presence of entanglements and mobility of the polymer chains. As a consequence, the lamellar thickness and radius of the spherulites shifted to small scales with increasing molecular weight while the crystal perfection turned to a low level. Moreover, for a given annealing condition, the trend of the melting temperature was also dependent on the molecular weight, suggesting the existence of different distribution of the lamellar thickness and the melting heat per unit volume in the various samples before the DSC scan. On the basis of various findings, we can conclude that (i) the long duration of the reaction redounds to enhance the encounter probabilities of the end groups inducing the increase of the average polymer chain length and molecular weight; (ii) the degree of crystalline perfection, the lamellar thickness, and the radius of the spherulites are found to strongly decrease with the increasing chain length due to the presence of the chain entanglements and the locomotor difficulty; (iii) the melting temperature is relevant to the molecular weight due to different lamellar thickness and melting heat per unit volume induced by mobility of the polymer chains. It seems that many morphological parameters such as lamellar thickness and radius of the spherulites are governed by the chain length and more directly by the mobility during its crystallization. Moreover, the melting behavior directly depends on the morphological parameters and thermodynamic parameters.

In balance, all the essentials lie on the molecular weight.

The authors thank Sun Lanhui for assistance with the experiment.

References

1. Attwood, T. E.; Dawson, P. C.; Freeman, J. L.; Hoy, L. R.; Rose, J. B.; Staniland, P. A. *Polymer* 1981, 22, 1096.
2. Stening, T. C.; Smith, C. P.; Kimber, P. J. *J Mod Plast* 1981, 58, 86.
3. Galli, E. *Plast Des Forum* 1985, March-April, 92.
4. Jones, D. P.; Leach, D. C.; Moore, D. R. *Polymer* 1985, 26, 1386.
5. Stening, T. C.; Smith, C. P.; Kimber, P. J. *Mod Plast* 1992, Int March, 54.
6. Vaughan, A. S.; Stevens, G. C. *Polymer* 1995, 36, 1531.
7. Jun, Y.; Aiqing, Z.; YongLiew, K.; Lihua, W. *Polym Bull* 2008, 61, 157.
8. John, B. R.; Philip, A. S. U.S. Pat. 4,320,224 (1982).
9. Labadie, J. W.; Hedrick, J. L.; Ueda, M. In *Step-Growth Polymers for High-Performance Materials—New Synthetic Methods*; Hedrick, J. L.; Labadie, J. W., Eds.; American Chemical Society: Washington, DC, 1996; Vol. 624, p 210.
10. Fougies, C.; Dosiere, M.; Koch, M. H. J.; Roovers, J. *Macromolecules* 1998, 31, 6266.
11. Blundell, D. J.; Osborn, B. N. *Polymer* 1983, 24, 953.
12. Kumar, S.; Anderson, D. P.; Adams, W. W. *Polymer* 1986, 27, 329.
13. Cebe, P.; Chung, S.; Hong, S. D. *J Appl Polym Sci* 1987, 33, 487.
14. Cho, B. R.; Kardos, J. L. *J Appl Polym Sci* 1995, 56, 1435.
15. Kong, Y.; Hay, J. N. *Polymer* 2002, 43, 3873.
16. Liang, M.; Lu, C.; Huang, Y.; Zhang, C. *J Appl Polym Sci* 2007, 106, 3895.
17. Rueda, D. R.; Ania, F.; Richardson, A.; Waxd, I. M.; Balta-Calleja, F. J. *Polym Commun* 1983, 24, 258.
18. Zimmermann, H. J.; Konneche, K. *Polymer* 1991, 32, 3162.
19. Iannelli, P. *Macromolecules* 1993, 26, 239.
20. Hsiao, B. S.; Gardner, K. H.; Wu, D. Q.; Chu, B. *Polymer* 1993, 34, 3986.
21. Jonas, A. M.; Russell, T. P.; Yoon, D. Y. *Macromolecules* 1996, 28, 8491.
22. Fougies, C.; Damman, P.; Villers, D.; Dosiere, M.; Koch, M. *Macromolecules* 1997, 30, 1385.
23. Naffakh, M.; Gomez, M. A.; Ellis, G.; Marco, C. *Polym Eng Sci* 2006, 46, 1411.
24. Meng, Y. Z.; Tjong, S. C. *J Appl Polym Sci* 2001, 81, 2687.
25. Salin, I. M.; Seferis, J. C. *J Appl Polym Sci* 1993, 47, 847.
26. Gupta, Y. N.; Chakraborty, A.; Pandey, G. D.; Setua, D. K. *J Appl Polym Sci* 2004, 92, 1737.
27. Hinkley, J. A.; Eftekhari, A.; Crook, R. A.; Jenson, B. J.; Singh, J. J. *J Polym Sci Part B Polym Phys* 1992, 30, 1195.
28. Lovinger, A. J.; Davis, D. D. *J Appl Polym Sci* 1985, 58, 2843.
29. Wang, J. K.; Yang, X. N.; Li, G.; Zhou, E. L. *J Appl Polym Sci* 2001, 82, 3431.
30. Zhang, Z.; Zeng, H. *Polymer* 1993, 34, 4032.
31. Gao, S. L.; Kim, J. K. *J Appl Polym Sci* 2002, 86, 478.
32. Yang, Y. H.; Zhu, W. C.; Jiang, D.; Ma, R. T.; Jiang, Z. H. *J Appl Polym Sci* 2007, 104, 35.
33. Chung, C. T.; Chen, M. *Polym Prepr* 1992, 33, 420.
34. Medellin-rodriguez, F. J.; Phillips, P. J. *Polym Eng Sci* 1996, 36, 703.
35. Ivanov, D. A.; Legras, R.; Jonas, A. M. *Polymer* 2000, 41, 3719.
36. William, G. K.; Bryan, B. S. *Polym Eng Sci* 2001, 41, 1714.
37. Yongsok, S.; Sehyun, K. *Polym Eng Sci* 2001, 41, 940.

38. Chiver, R. A.; Moore, D. R. *Polymer* 1994, 35, 110.
39. Ke, Y. C.; Wu, Z. W. *J Appl Polym Sci* 1998, 67, 2065.
40. Page, D. J. Y. S.; Bonin, H. W.; Bui, V. T.; Bates, P. J. *J Appl Polym Sci* 2002, 86, 2713.
41. Mallakpour, S.; Khani, M.; Rafiemanzelat, F. *J Appl Polym Sci* 2008, 108, 3038.
42. Manjun, H.; Weixiao, C.; Xixia, D. *Physics of Polymer*; Fudan Press: Shanghai, 2006.
43. Namazi, H.; Rad, S. J. *J Appl Polym Sci* 2004, 94, 1175.
44. Zhishen, M.; Hongfang, Z. *Structure of Crystalline Polymer and X-ray Diffraction*; Science Press: Beijing, 2003.
45. Marega, C.; Causin, V.; Marigo, A. *J Appl Polym Sci* 2008, 109, 32.
46. Reyna-Valencia, A.; Kaliaguine, S.; Bousmina, M. *J Appl Polym Sci* 2006, 99, 756.
47. Muellerleile, J. T.; Freeman, J. J. *J Appl Polym Sci* 1994, 54, 135.
48. Rao, V. L.; Sivadasan, P. *Eur Polym J* 1994, 30, 1381.